Transient time-domain resonances and the time scale for tunneling

Gastón García-Calderón[1,*] and Jorge Villavicencio[2,†]
[1]*Instituto de Física, Universidad Nacional Autónoma de México, Apartado Postal 20 364, 01000 México, Distrito Federal, Mexico*
[2]*Facultad de Ciencias, Universidad Autónoma de Baja California, Apartado Postal 1880, 22800 Ensenada, Baja California, Mexico*
(Received 20 November 2002; revised manuscript received 25 August 2003; published 17 November 2003)

Transient *time-domain resonances* found recently in time-dependent solutions to Schrödinger's equation are used to investigate the issue of the tunneling time in rectangular potential barriers. In general, a time-frequency analysis shows that these transients have frequencies above the cutoff frequency associated with the barrier height, and hence correspond to nontunneling processes. We find, however, a regime characterized by the barrier opacity, where the peak maximum t_{max} of the time-domain resonance corresponds to under-the-barrier tunneling. We argue that t_{max} represents the relevant tunneling time scale through the classically forbidden region.

DOI: 10.1103/PhysRevA.68.052107 PACS number(s): 03.65.Xp, 03.65.Ca, 73.40.Gk

Tunneling refers to the possibility that a particle traverses through a classically forbidden region. In the energy domain the solution to Schrödinger's equation at a fixed energy E is a subject discussed in every quantum mechanics textbook. In the time domain, however, there are still aspects open to scrutiny. A problem that has remained controversial over the years is the tunneling time problem that may be stated by the question: How long does it take to a particle to traverse a classically forbidden region? Different authors have proposed and defended different views in answering the above question [1–4].

In a recent work we have investigated the effect of the transient solutions to the time-dependent Schrödinger's equation for cutoff wave initial conditions (quantum shutter) on the tunneling process [5–7]. In particular we found that just across the tunneling barrier, the probability density as a function of time may exhibit a transient structure that we have named time-domain resonance. The peak value t_{max} of this structure represents the largest probability of finding the particle at the barrier width L. More recently, in collaboration with Delgado and Muga [8], we considered a time-frequency analysis [9,10] to show the existence of under-the-barrier transients (forerunners) in very broad barriers. However, these occur along a finite region of the potential, and hence do not allow to characterize the time scale associated with the tunneling process through the full classically forbidden region. On the other hand, in collaboration with Yamada [11] we have recently established the equivalence of our formulation with the notion of ''passage time'' in the real Feynman histories approach. The passage time yields the traversal time through a barrier region though it does not distinguish between processes from above or below the barrier height. The above considerations indicate that it is not clear under what conditions the time-domain resonances found at the barrier edge $x=L$ correspond to genuine tunneling processes.

The aim of this work is to show the existence of a regime, characterized by the opacity of the system, where the time-domain resonance maximum t_{max} corresponds to under-the-barrier tunneling. We argue that this time scale provides the tunneling time through the classically forbidden region.

Our approach to the tunneling time problem is based on a model that deals with an explicit solution [5] to the time-dependent Schrödinger's equation

$$\left[i\hbar \frac{\partial}{\partial t} + \frac{\hbar^2}{2m} \frac{\partial^2}{\partial x^2} - V(x) \right] \Psi(x,t) = 0 \tag{1}$$

for an arbitrary potential $V(x)$, defined in the region $(0 \leqslant x \leqslant L)$, that vanishes outside that region. We consider the problem of the time evolution of a cutoff plane wave

$$\Psi(x,t=0) = \begin{cases} e^{ikx} - e^{-ikx}, & x \leqslant 0 \\ 0, & x > 0, \end{cases} \tag{2}$$

following the instantaneous opening at $t=0$ of a quantum shutter at $x=0$. Along the tunneling region the solution reads

$$\Psi^i(x,k;t) = \phi_k(x) M(y_k) - \phi_{-k}(x) M(y_{-k}) - \sum_{n=-\infty}^{\infty} \phi_n(x) M(y_{k_n}) \quad (0 \leqslant x \leqslant L), \tag{3}$$

where the $\phi_{\pm k}(x)$'s refer to the stationary solutions of the problem and $\phi_n(x) = 2iku_n(0)u_n(x)/(k^2 - k_n^2)$. Similarly, the solution $\Psi^e(x,k;t)$ for the external or transmitted region $(x \geqslant L)$ is given by [6]

$$\Psi^e(x,k;t) = T_k M(y_k) - T_{-k} M(y_{-k}) - i \sum_{n=-\infty}^{\infty} T_n M(y_{k_n}) \quad (x \geqslant L), \tag{4}$$

where the $T_{\pm k}$'s refer to the transmission amplitudes and the factor $T_n = 2iku_n(0)u_n(L)\exp(-ik_nL)/(k^2 - k_n^2)$. In Eqs. (3) and (4) the coefficients χ_n and T_n are given in terms of the resonant eigenfunctions $\{u_n(x)\}$ with complex energy eigenvalues $E_n = \hbar^2 k_n^2/2m$, with $k_n = a_n - ib_n$ $(a_n, b_n > 0)$. The resonant sums in Eqs. (3) and (4) run over the full set of complex poles $\{k_n\}$. The M's are defined as [5]

*Electronic address: gaston@fisica.unam.mx
†Electronic address: villavics@uabc.mx

 ©2003 The American Physical Society

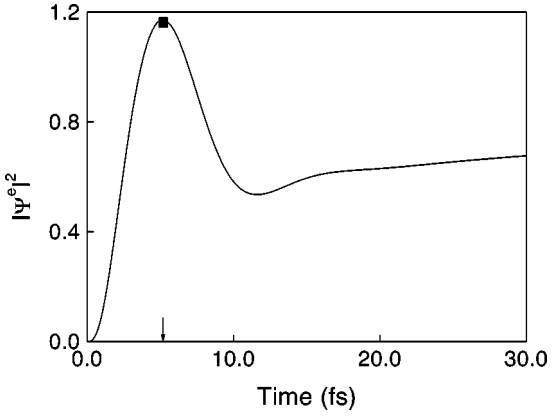

FIG. 1. Time evolution of $|\Psi^e|^2$ (solid line) at $x=L=4.0$ nm. A full square indicates the position of the maximum of the time-domain resonance at $t_{max}=5.17$ fs.

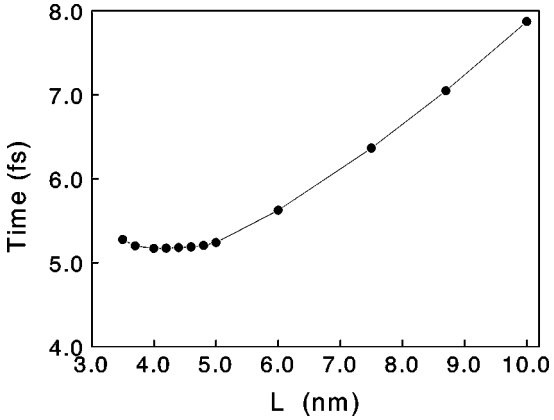

FIG. 2. Maximum of the time-domain resonance t_{max} (full dot) as a function of the barrier width L for an incidence energy $E=0.001$ eV. In this case the barrier height is $V=0.3$ eV. See text.

$$M(y_q)=\tfrac{1}{2}e^{imx^2/2\hbar t}w(iy_q), \tag{5}$$

where w is the complex error function [12] defined as $w(z)=\exp(-z^2)\mathrm{erfc}(-iz)$ with arguments $y_q(x,t)=e^{-i\pi/4}(m/2\hbar t)^{1/2}[x-\hbar qt/m]$, where $q=\pm k,\ k_n$.

We shall begin exploring the issue of the tunneling time scale by first considering specific examples of rectangular potential barriers (of height V and thickness L) to go then to results of a more general character. Let us recall the main features of a time-domain resonance [6]. It follows from the initial condition, given by Eq. (2), that initially there is no particle along the tunneling region. Hence evaluating the probability density at the barrier width $x=L$ as time evolves from zero yields a distribution of characteristic times associated with the tunneling process. In Fig. 1 we plot the probability density $|\Psi^e|^2$ (solid line), normalized to the transmission coefficient $|T_k|^2$, as a function of time t, corresponding to a potential barrier system with typical parameters [13]: $V=0.3$ eV, incidence energy $E=\hbar^2k^2/2m=0.001$ eV, and effective mass for the electron $m=0.067m_e$, for a fixed value of position $x=L=4.0$ nm. We can clearly appreciate a structure peaked at the value $t_{max}=5.17$ fs. This is the so-called time-domain resonance.

In Fig. 2 we plot t_{max} (full dot) for the same parameters as in Fig. 1 except for the barrier width L that we vary. Here we can clearly observe the existence of a basin along a range of values of the barrier width. We can also appreciate that if L is further increased, t_{max} starts to grow linearly with L. Such a linear regime occurs at large barrier widths. We have discussed elsewhere that this last situation refers to nontunneling processes [6]. We have also pointed out in Ref. [6] that for small values of the barrier width L, the basin exhibited by t_{max} is the result of a subtle interplay between tunneling and (nontunneling) top-barrier resonant processes.

In what follows we shall investigate under what conditions the time scales associated with the basin, are in fact related to a genuine tunneling process.

We use the fact that the initial cutoff wave possesses a distribution of momentum components in k space, and hence also of frequency components. As time evolves and the wave interacts with the potential, these frequency components manifest themselves in the time evolution of the probability density. The frequency content of the time-domain resonance can be investigated by performing a time-frequency analysis. We do this by computing the local average frequency ω_{av} [9,10],

$$\omega_{av}=-\mathrm{Im}\left[\frac{1}{\Psi^s}\frac{d}{dt}\Psi^s\right], \tag{6}$$

and the instantaneous bandwidth σ [10]

$$\sigma=\left|\mathrm{Re}\left[\frac{1}{\Psi^s}\frac{d}{dt}\Psi^s\right]\right|, \tag{7}$$

where $s=i$ and e refers, respectively, to the internal and external solutions. To exemplify this, we choose the case $L=4.0$ nm depicted in Fig. 2, which is located around the minimum of the basin. In Fig. 3 we plot the relative average local frequency (relative frequency for short) ω_{av}/ω_V,

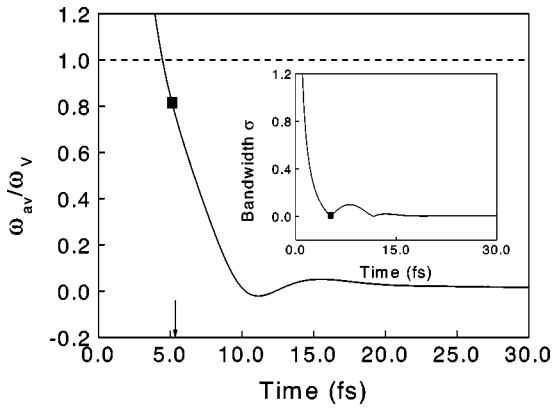

FIG. 3. Relative average local frequency ω_{av}/ω_V (solid line) for the case depicted in Fig. 1. The cutoff frequency $\omega_{av}/\omega_V=1$ (dashed line) is included for comparison. In the inset we plot the instantaneous bandwidth σ of the spectrogram depicted in the main graph. Notice that the frequency deviations at t_{max} are exactly zero, i.e., $\sigma(t_{max})=0$. In all cases a full square indicates the position of t_{max}.

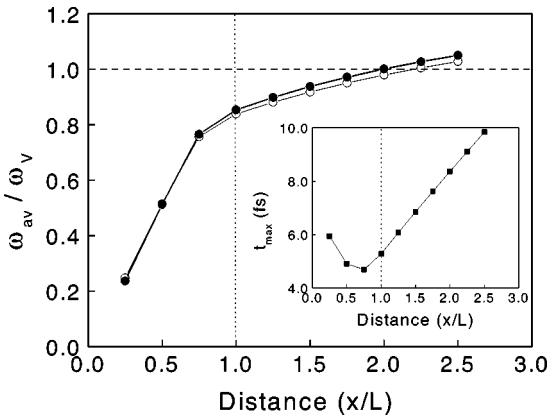

FIG. 4. Relative frequency ω_{av}/ω_V of the maximum of the time-domain resonance as a function of position, measured in units of the barrier width L. The parameters are given in the text. Two incidence energies are considered: $E=0.001$ eV (solid dot) and $E=0.01$ eV (hollow dot). In both cases, the relative frequency ω_{av}/ω_V along the internal region is below the cutoff frequency $\omega_{av}/\omega_V=1$ (dashed line). The behavior of t_{max} as a function of position is illustrated in the inset for the case with $E=0.01$ eV. The position of the barrier edge, $x=L$, is indicated by a dotted line in both figures.

where $\omega_V=V/\hbar$ is the cutoff frequency, along the relevant time interval, discussed in Fig. 1. We can appreciate that in the vicinity of the maximum of the time-domain resonance t_{max} the probability density is composed entirely of under-the-barrier frequency components, i.e., $\omega_{av}/\omega_V<1$. This also occurs at the exact value t_{max}, also indicated in the figure by a solid square. In the inset of Fig. 3 we plot the instantaneous bandwidth σ of the spectrogram. Notice the absence of a frequency dispersion around the maximum t_{max}, i.e., $\sigma(t_{max})=0$. The above result indicates that in this case the peak of the time-domain resonance and the values close to it refer to a tunneling event. We have found, however, that this is not a general situation. For instance, for values of L outside the basin, i.e., along the linear regime in Fig. 2, the average frequency related to the corresponding t_{max} is above the cutoff frequency and hence refers to nontunneling processes. As we shall present below this is more appropriately discussed by using the notion of the opacity of the system. In Fig. 4 we plot the relative frequency ω_{av}/ω_V associated with different values of the maximum t_{max}, measured at different positions along both the internal and external regions of a potential barrier with parameters: $V=0.3$ eV and $L=4.13$ nm. In this case we choose the following values of the incidence energy: $E=0.001$ eV (solid dot) and $E=0.01$ eV (hollow dot). In the inset of Fig. 4 we show, for the particular case of $E=0.01$ eV, the values of t_{max} (solid square) at the different values of position considered in the main graph. As can be clearly appreciated in that figure, the tunneling process along the whole internal region is governed by under-barrier-frequency components, i.e., $\omega_{av}/\omega_V<1$. We can see in Fig. 4 that we can still observe frequency components below the cutoff frequency ω_V for distances up to $x\simeq 2L$ along the external region. As x/L increases further, $\omega_{av}/\omega_V>1$. This behavior indicates the prevalence of nontunneling components in the behavior of the probability density [7].

We have found that the regime which corresponds to under-the-barrier time-domain resonances at the barrier edge $x=L$ may be described more generally by referring to the opacity α of the system, defined as

$$\alpha=\frac{[2mV]^{1/2}}{\hbar}L, \tag{8}$$

and by the dimensionless parameter u, the ratio between the potential barrier height and the incidence energy:

$$u=\frac{V}{E}. \tag{9}$$

To characterize this tunneling regime, we use the fact that all systems sharing the same parameters α and u yield the same relative frequency ω_{av}/ω_V. This regularity arises from a simple rescaling property of the time-dependent Schrödinger's equation and the corresponding initial condition. By feeding the dimensionless variables $X=x/L$ and $T=\omega_V t$ in Eqs. (1) and (2), we obtain

$$\left[i\frac{\partial}{\partial T}+\frac{1}{\alpha^2}\frac{\partial^2}{\partial X^2}-1\right]\chi(X,T)=0, \tag{10}$$

with the initial condition

$$\chi(X,T=0)=\begin{cases} e^{i\alpha X/\sqrt{u}}-e^{-i\alpha X/\sqrt{u}}, & X\leqslant 0 \\ 0, & X>0, \end{cases} \tag{11}$$

where $\chi(X,T)$ is the rescaled time-dependent solution. From Eqs. Eqs. (10) and (11), it is clear that the time-dependent solution must depend only on the parameters α and u that is, for a fixed value of α, all the systems with the same parameter u yield the same $\chi(X,T)$. As a consequence of the above considerations we can write the relative frequency as

$$\frac{\omega_{av}}{\omega_V}=-\mathrm{Im}\left[\frac{1}{\chi}\frac{d}{dT}\chi\right]. \tag{12}$$

and use it to characterize the regime associated with under-the-barrier frequency components. In particular, we are interested in defining the range of values of α where the relative frequencies associated with the time-domain resonance are below the cutoff frequency ω_V. In Ref. [7] it is found that for opacities less than a critical value no time domain resonances occur. We denote it by α_{min} and it has the value $\alpha_{min}=2.065$. In Fig. 5 we plot the relative frequency ω_{av}/ω_V as a function of the opacity α for three different values of the parameter u: $u=5$ (solid dot), $u=10$ (solid triangle), and $u=300$ (solid square). In this case we have chosen a value of $V=0.3$ eV in the calculation. Although in Fig. 5 we have considered values of the parameter u such that $5\leqslant u\leqslant 300$, the cases corresponding to very large values of u ($u\to\infty$) (not shown here) almost overlap with the case

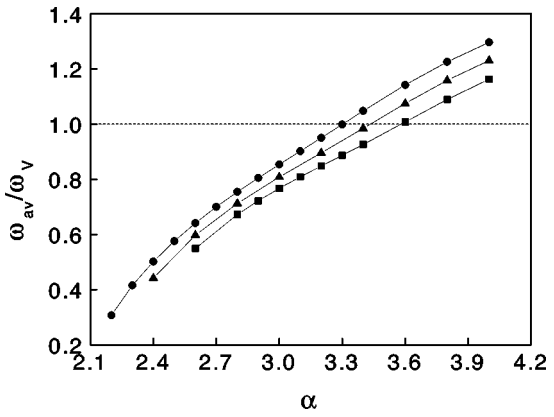

FIG. 5. Relative frequency ω_{av}/ω_V measured at the barrier edge $x=L$, as a function of the opacity α. Here we considered a barrier height $V=0.3$ eV, and the parameters: $u=300$ (solid dot), $u=10$ (solid triangle), and $u=5$ (solid square). Note that for values of the opacity smaller than $\alpha\simeq 3.3$, the relative frequencies for all values of u are below the cutoff frequency $\omega_{av}/\omega_V=1$ (dashed line). See text.

$u=300$. Thus, for very large values of u we find a maximum value for the opacity $\alpha_{max}\sim 3.3$. Consequently one may define an opacity "window," in the range of values $2.065\leqslant\alpha\leqslant 3.3$, where the relative frequencies are always below the cutoff frequency $\omega_{av}/\omega_V=1$, irrespective of the value of the parameter u, namely, of the value of the incidence energy. Note that the above numerical values refer to the effective mass $m=0.067m_e$ and clearly will be modified for other values of the effective mass.

It is of relevance to point out that along the basin region the time scale given by the peak maximum t_{max} differs in a essential way from both the semiclassical Büttiker-Landauer and Büttiker traversal times, which in addition to exhibit always a linear dependence with L, refer to over-the-barrier processes [9,6]. Also t_{max} represents a completely different notion than the phase time, which corresponds to a long-time asymptotic notion representing a global effect of the potential on the Schrödinger's solution, as discussed in Refs. [6,7].

To conclude we remark that the analytical solution to the time-dependent Schrödinger's equation with quantum shutter initial conditions applies in general to arbitrary potentials, provided they vanish beyond a distance, and can also be extended to deal with finite cutoff pulses as discussed in Ref. [7]. The quantum shutter setup provides a consistent procedure to obtain the tunneling time: initially there is no particle along the tunneling region and as time evolves the transient peaked structure exhibited by the probability density at the barrier width provides the relevant time scale for tunneling. This occurs within a range of values of the opacity of the system and is independent of the incidence energy. It is worth noticing that the values of α within the opacity "window" may be obtained using typical parameters of semiconductor heterostructures [13]. Also one should stress that at the peak maximum, the time-domain resonance is governed by a single frequency, that is, the system acts as a frequency filter. To test our results experimentally would require to consider the detection of tunneling particles in time domain at distances close to the interaction region.

The authors thank J. G. Muga for useful discussions and a critical reading of the manuscript, and acknowledge financial support from DGAPA-UNAM under Grant No. IN101301.

[1] E.H. Hauge and J.A. Støvneng, Rev. Mod. Phys. **61**, 917 (1989).
[2] R. Landauer and Th. Martin, Rev. Mod. Phys. **66**, 217 (1994).
[3] P. Ghose, *Testing Quantum Mechanics on New Ground* (Cambridge University Press, Cambridge, 1999), Chap. 10.
[4] *Time in Quantum Mechanics*, edited by J.G. Muga, R. Sala, and I.L. Egusquiza (Springer-Verlag, Berlin, 2002).
[5] G. García-Calderón and A. Rubio, Phys. Rev. A **55**, 3361 (1997).
[6] G. García-Calderón and J. Villavicencio, Phys. Rev. A **64**, 012107 (2001).
[7] G. García-Calderón and J. Villavicencio, Phys. Rev. A **66**, 032104 (2002).
[8] G. García-Calderón, J. Villavicencio, F. Delgado, and J.G. Muga, Phys. Rev. A **66**, 042119 (2002).
[9] J.G. Muga and M. Büttiker, Phys. Rev. A **62**, 023808 (2000).
[10] L. Cohen, *Time-Frequency Analysis* (Prentice Hall, New Jersey, 1995).
[11] G. García-Calderón, Jorge Villavicencio, and N. Yamada, Phys. Rev. A **67**, 052106 (2003).
[12] *Handbook of Mathematical Functions*, edited by M. Abramowitz and I.A. Stegun (Dover, New York, 1965), p. 297.
[13] E.E. Mendez, in *Physics and Applications of Quantum Wells and Superlattices*, edited by E.E. Mendez and K. Von Klitzing (Plenum, New York, 1987), p. 159; D.K. Ferry and S.M. Goodnick, *Transport in Nanostructures* (Cambridge University Press, Cambridge, 1997), pp. 91–201.